DALTON
FULL PAPER

Transition-metal imido-boroxide complexes: a structural and spectroscopic investigation of the influence of boron

Sarah C. Cole, Martyn P. Coles* and Peter B. Hitchcock

Department of Chemistry, University of Sussex, Falmer, Brighton, UK BN1 9QJ.
E-mail: m.p.coles@sussex.ac.uk.

Received 24th July 2002, Accepted 10th September 2002
First published as an Advance Article on the web 21st October 2002

The four coordinate compounds $Mo(NR)_2[OB(mes)_2]_2$ (**1**, R = ^{t}Bu; **2**, R = Ar = 2,6-^{i}Pr$_2$C$_6$H$_3$) have been obtained from the reaction of $[(mes)_2BOLi(Et_2O)_n]_x$ with the corresponding $Mo(NR)_2Cl_2(dme)$ starting material; for structural comparison, $Mo(N^tBu)_2[OCH(mes)_2]_2$ (**3**) was also synthesised. The related five-coordinate complexes $Ti(N^tBu)[OB(mes)_2]_2(py)_2$ (**4**) and $Ti(N^tBu)[OCH(mes)_2]_2(py)_2$ (**5**) were made using analogous procedures. X-Ray structural investigations of **1**–**5** were performed to assess the effect that the boron atom has on the metal–oxygen and metal–nitrogen(imido) bond lengths and angles. On average, both classes of compound displayed longer metal–oxygen bonds and shorter metal–nitrogen(imido) bonds for the boroxide derivatives. Spectroscopic investigation of the $\Delta\delta$ values for the *tert*-butylimido derivatives revealed that complexes incorporating the $[OB(mes)_2]^-$ anion exhibit a reduction in the electron density at the imido nitrogen atom, in agreement with the observations from the solid state structures.

1 Introduction

Alkoxide and aryloxide ligands have played a prominent role in coordination chemistry during the past 30 years.[1] The properties which these ligands impart to the complex can be varied through derivatisation of the alkyl and aryl substituents, leading to their application in a range of catalytic processes. Frequently, sterically bulky groups are employed in these systems in order to limit the aggregation to molecular species that are more amenable to study. Each ligand type is capable of coordinating to a transition-metal centre as a [1σ, 2π] donor group, able to contribute up to five electrons to the metal centre.[2] The extent of π-donation that occurs from the oxygen lone-pairs can be influenced by the nature of the substituents, which can have a profound effect on the chemistry observed at the metal centre. For example, the introduction of electron withdrawing (fluorinated) substituents in the molybdenum alkylidene complexes $Mo(NAr)(CHR)(OR')_2$ results in dramatically different reactivity with respect to catalytic olefin metathesis.[3]

An alternative approach to controlling the extent of π-donation from alkoxide-type ligands is by the incorporation of an atom with an empty π-acceptor orbital adjacent to the O-atom. This has previously been the subject of a brief study for boron-substituted alkoxide (boroxide) ligands, where the empty 2p-orbital on boron is accessible for donation from the oxygen lone pairs. Power and co-workers reported a series of late transition-metal compounds, showing that ligands of the type $[R_2BO]^-$ (R = mes = 2,4,6-Me$_3$C$_6$H$_2$; 2,4,6-^{i}Pr$_3$C$_6$H$_2$) are able to adopt either a bridging or terminal coordination mode (Fig. 1).[4,5] Additional work by Gibson and co-workers sought to enhance this effect through the introduction of the fluorinated-mesityl derivative, 2,4,6-(CF$_3$)$_3$C$_6$H$_2$ (Fmes) at boron, and concluded that a greater localisation of electron density was present in the B–O bond, from a structural comparison of $[(Fmes)_2BOLi(THF)]_2$ with the non-fluorinated mesityl analogue.[6] We have initiated a study into the application of these, and related boron–oxygen ligands in early transition-metal chemistry,[7] and present in this publication a structural and spectroscopic study comparing the bonding of $[(mes)_2BO]^-$ with the sterically similar, 'conventional' alkoxide $[(mes)_2CHO]^-$ in molybdenum- and titanium-imido complexes.

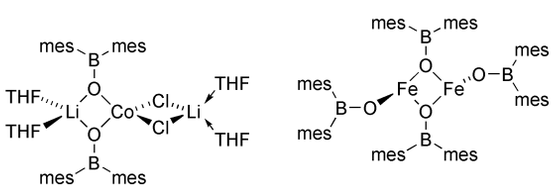

Fig. 1

2 Experimental

General experimental procedures

All manipulations were carried out under dry nitrogen using standard Schlenk and cannula techniques, or in a conventional nitrogen-filled glovebox. Solvents were dried over the appropriate drying agent and degassed prior to use. The compounds $(mes)_2BOH$,[8] $(mes)_2CHOH$,[9] $Mo(NR)_2Cl_2(dme)$, (R = ^{t}Bu, Ar = 2,6-^{i}Pr$_2$C$_6$H$_3$)[10] and $Ti(N^tBu)Cl_2(py)_3$,[11] were synthesised according to literature procedures.

Elemental analyses were performed by S. Boyer at the University of North London. NMR spectra were recorded using a Bruker Avance DPX 300 MHz spectrometer. Coupling constants are quoted in Hz.

$Mo(N^tBu)_2[OB(mes)_2]_2$ (1)

^{n}BuLi (1.6 mL of a 2.5 M solution in hexane, 4.00 mmol) was added *via* syringe to a solution of $(mes)_2BOH$ (1.00 g, 3.76 mmol) in Et$_2$O (25 mL) at 0 °C. The resultant mixture was allowed to warm to ambient temperature and was stirred for 1 h, during which time a fine white precipitate formed. The slurry was added to a solution of $Mo(N^tBu)_2Cl_2(dme)$ (0.75 g, 1.88 mmol) in Et$_2$O (40 mL) that had been cooled to −78 °C. Upon warming, a dark green solution and an off-white precipitate formed, which was stirred at room temperature for 14 h. The volatiles were removed under reduced pressure and the resultant green solid extracted from LiCl with hexane. Concentration and storage at −30 °C yielded **1** as yellow-green crystals. Yield 0.76 g (53%).

 DOI: 10.1039/b207277g

Anal. calc. for $C_{44}H_{62}N_2B_2MoO_2$: C, 68.76; H, 8.13; N, 3.64. Found: C, 68.92; H, 8.23; N, 3.52%. ^{1}H NMR (C_6D_6, 298 K): δ 6.73 (s, 8H, C_6H_2), 2.45 (s, 24H, 2,6-Me_2), 2.14 (s, 12H, 4-Me), 1.08 (s, 18H, $NCMe_3$). ^{13}C NMR (C_6D_6, 298 K): δ 141.1 (CH), 138.1 (C), 128.7 (C), 128.6 (C), 71.0 ($NCMe_3$), 31.6 ($NCMe_3$), 23.2 (2,6-Me_2) 21.2 (4-Me). MS (EI^+, *m*/*z*) 769 $[M]^+$.

$Mo(NAr)_2[OB(mes)_2]_2$ (2)

^{n}BuLi (0.9 mL of a 2.5 M solution in hexane, 2.25 mmol) was added *via* syringe to a solution of $(mes)_2BOH$ (0.60 g, 2.25 mmol) in Et_2O (20 mL) at 0 °C. The resultant mixture was allowed to warm to ambient temperature and was stirred for 1 h, during which time a fine white precipitate formed. The slurry was added to a solution of $Mo(NAr)_2Cl_2$(dme) (0.68 g, 1.12 mmol) in Et_2O (30 mL) that had been cooled to −78 °C, affording a red solution and a yellow precipitate, which was stirred at room temperature for 14 h. The volatiles were removed under reduced pressure, and the resultant red solid was extracted from LiCl with pentane. Concentration and storage at −30 °C yielded **2** as red crystals. Yield 0.71 g (65%).

Anal. calc. for $C_{60}H_{78}N_2B_2MoO_2$: C, 74.60; H, 8.14; N, 2.90. Found: C, 74.59; H, 8.25; N, 2.83%. ^{1}H NMR (C_6D_6, 298 K): δ 6.89 (mult, 6H, C_6H_3), 6.66 (s, 8H, C_6H_2), 3.62 (sept, $^3J_{HH}$ = 6.9, 4H, $CHMe_2$), 2.41 (s, 24H, 2,6-Me_2), 2.13 (s, 12H 4-Me), 0.97 (d, $^3J_{HH}$ = 6.9, 24H $CHMe_2$). ^{13}C NMR (C_6D_6, 298 K): δ 154.2 (C), 143.1 (C), 141.0 (C), 139.4 (br, C), 138.4 (C), 128.8 (CH), 127.3 (CH), 123.0 (CH), 28.7 ($CHMe_2$), 23.7 (CH_3), 23.1 (CH_3), 21.3 (CH_3). MS (EI^+, *m*/*z*) 978 $[M]^+$.

$Mo(N^tBu)_2[OCH(mes)_2]_2$ (3)

^{n}BuLi (0.6 mL of a 2.5 M solution in hexane, 1.50 mmol) was added *via* syringe to a solution of $(mes)_2CHOH$ (0.40 g, 1.49 mmol) in Et_2O (20 mL) at 0 °C. The resultant mixture was allowed to warm to ambient temperature and was stirred for 1 h, during which time a fine white precipitate formed. The slurry was added to a solution of $Mo(N^tBu)_2Cl_2$(dme) (0.30 g, 0.75 mmol) in Et_2O (25 mL) that had been cooled to −78 °C, affording a brown solution and a white precipitate which was stirred at room temperature for 14 h. The volatiles were removed under reduced pressure, and the resultant brown solid was extracted from LiCl with hexane. Concentration and cooling to −30 °C yielded **3** as colourless crystals. Yield 0.34 g (61%).

Anal. calc. for $C_{46}H_{64}N_2MoO_2$: C, 71.48; H, 8.35; N, 3.62. Found: C, 71.45; H, 8.41; N, 3.54%. ^{1}H NMR (C_6D_6, 298 K): δ 7.33 (s, 2H, CHO), 6.70 (s, 8H, C_6H_2), 2.36 (s, 24H, 2,6-Me_2), 2.13 (s, 12H, 4-Me), 1.20 (s, 18H, $NCMe_3$). ^{13}C NMR (C_6D_6, 298 K): δ 138.3 (CH), 137.1(C), 136.0 (C), 130.9 (C), 88.2 (CHO), 69.6 ($NCMe_3$), 32.4 ($NCMe_3$), 22.0 (CH_3), 20.9 (CH_3).

$Ti(N^tBu)[OB(mes)_2]_2(py)_2$ (4)

^{n}BuLi (0.8 mL of a 2.5 M solution in hexane, 2.00 mmol) was added *via* syringe to a solution of $(mes)_2BOH$ (0.50 g, 1.88 mmol) in Et_2O (25 mL) at 0 °C. The resultant mixture was allowed to warm to ambient temperature and was stirred for 1 h, during which time a fine white precipitate formed. The slurry was added to a solution of $Ti(N^tBu)Cl_2(py)_3$ (0.40 g, 0.94 mmol) in Et_2O (25 mL) that had been cooled to −78 °C, affording a yellow solution which was stirred at room temperature for 14 h. The volatiles were removed under reduced pressure, and the resultant brown solid was extracted with hexane and filtered. Concentration and storage at −4 °C yielded **3** as yellow crystals. Yield 0.41 g (53%).

Anal. calc. for $C_{50}H_{63}N_3B_2O_2Ti$: C, 74.37; H, 7.86; N, 5.20. Found: C, 74.38; H, 7.73; N, 5.30%. ^{1}H NMR ($CDCl_3$, 298 K): δ 8.62 (d, br, $^2J_{HH}$ = 4.8, 4H, pyridine-H_{ortho}), 7.49 (t, br, 2H, pyridine-H_{para}), 6.83 (t, br, 4H, pyridine-H_{meta}), 6.56 (2, 8H, C_6H_2), 2.20 (s, 12H, 4-Me), 2.13 (s, 24H, 2,6-Me_2), 0.77 (s, 9H, $NCMe_3$). ^{13}C NMR ($CDCl_3$, 298 K): δ 150.4 (CH), 142.1 (br, C), 140.2 (C), 136.9 (C), 135.9 (CH), 127.4 (CH), 123.0 (CH), 69.6 (C), 31.6 (CH_3), 22.6 (CH_3), 21.1 (CH_3). MS (EI^+, *m*/*z*): 1178 [dimer − (mes)]$^+$, 914 [dimer − $[OB(mes)_2]$ − (mes)]$^+$, 842 [dimer − (N^tBu) − $[OB(mes)_2]$ − (mes)]$^+$ (where dimer = $\{Ti(N^tBu)[OB(mes)_2]_2\}_2$, believed to form by combination of molecular fragments upon loss of pyridine).

$Ti(N^tBu)[OCH(mes)_2]_2(py)_2$ (5)

^{n}BuLi (0.6 mL of a 2.5 M solution in hexane, 1.50 mmol) was added *via* syringe to a solution of $(mes)_2CHOH$ (0.40 g, 1.49 mmol) in Et_2O (25 mL) at 0 °C. The resultant mixture was allowed to warm to ambient temperature and was stirred for 1 h, during which time a fine white precipitate formed. The slurry was added to a solution of $Ti(N^tBu)Cl_2(py)_3$ (0.32 g, 0.75 mmol) in Et_2O (25 mL) that had been cooled to −78 °C, affording a yellow solution which was stirred at room temperature for 14 h. The volatiles were removed under reduced pressure, and the resultant yellow solid was extracted with hexane and filtered. Concentration and storage at −4 °C yielded **5** as yellow crystals. Yield 0.42 g (70%).

Anal. calc. for $C_{50}H_{63}N_3B_2O_2Ti$: C, 76.92; H, 8.08; N, 5.18. Found: C, 77.02; H, 8.14; N, 5.19%. ^{1}H NMR ($CDCl_3$, 298 K): δ 8.47 (d, br, $^2J_{HH}$ = 4.5, 4H, pyridine-H_{ortho}), 7.53 (t, $^2J_{HH}$ = 7.6, 2H, pyridine-H_{para}), 7.27 (s, 2H, CHO), 7.02 (t, $^2J_{HH}$ = 6.6, 4H, pyridine-H_{meta}), 6.57 (s, 8H, C_6H_2), 2.16 (s, 12H, 4-Me), 2.13 (s, 24H, 2,6-Me_2), 0.77 (s, 9H, $NCMe_3$). ^{13}C NMR ($CDCl_3$, 298 K): δ 150.3 (CH), 140.4 (C), 136.3 (C), 136.1 (CH), 134.1 (C), 129.6 (CH), 122.8 (CH), 81.4 (CH), 67.1 (C), 32.1 (CH_3), 21.2 (CH_3), 20.4 (CH_3).

Crystallography

Details of the crystal data, intensity collection and refinement for complexes **1**, **2** and **3** are listed in Table 1, and for complexes **4** and **5** in Table 2. Crystals were covered in oil and suitable single crystals were selected under a microscope and mounted on a Kappa CCD diffractometer. The structures were refined with SHELXL-97.[12] Additional features are described below.

CCDC reference numbers 190539–190543.

See http://www.rsc.org/suppdata/dt/b2/b207277g/ for crystallographic data in CIF or other electronic format.

$Mo(N^tBu)_2[OB(mes)_2]_2$ (**1**). The molecule lies on a 2-fold rotation axis.

$Mo(NAr)_2[OB(mes)_2]_2$ (**2**). Two independent molecules are present in the unit cell with slight differences in bond lengths and angles.

$Ti(N^tBu)[OB(mes)_2]_2(py)_2$ (**4**). The complex crystallises with half a molecule of hexane in the unit cell.

$Ti(N^tBu)[OCH(mes)_2]_2(py)_2$ (**5**). Two independent molecules are present in the unit cell with slight differences in bond lengths and angles.

3 Results and discussion

The lithium salt of dimesitylborinic acid has previously been isolated as the mono-THF solvate, $[(mes)_2BOLi(THF)]_2$, in near quantitative yields.[4] For the purposes of our investigations we found it convenient to generate the salt *in situ* as a fine, white powder, that could be easily added as a suspension (in diethyl ether) to the appropriate metal-chloride salt. Thus, 2 equivalents of $[(mes)_2BOLi(Et_2O)_n]_x$, were reacted with $Mo(N^tBu)_2Cl_2$(dme) at low temperature to afford $Mo(N^tBu)_2[OB(mes)_2]_2$ (**1**) as green-yellow crystals (Scheme 1). The bis(arylimido) derivative, $Mo(NAr)_2[OB(mes)_2]_2$ (**2**, Ar = 2,6-$^i Pr_2C_6H_3$), was isolated as red crystals from the analogous reaction using the appropriate starting material. In both cases, NMR, mass spectral and elemental analytical data were consistent with the molybdenum bis(imido)bis(boroxide) complex. In order to help to determine the influence of the boron substituent on the

Table 1 Crystal structure and refinement data for **1**, **2** and **3**

	1	**2**	**3**
Formula	$C_{44}H_{62}B_2MoN_2O_2$	$C_{60}H_{78}B_2MoN_2O_2$	$C_{46}H_{64}MoN_2O_2$
Formula weight	768.52	976.80	772.93
Temperature/K	173(2)	173(2)	173(2)
Wavelength/Å	0.71073	0.71073	0.71073
Crystal size/mm	0.4 × 0.3 × 0.3	0.2 × 0.2 × 0.1	0.3 × 0.3 × 0.2
Crystal system	Orthorhombic	Orthorhombic	Monoclinic
Space group	*Aba*2 (no. 41)	$Pbc2_1$ (no. 29)	$P2_1/n$ (no. 14)
a/Å	19.0505(6)	13.2134(4)	19.4544(3)
b/Å	27.3517(7)	19.0999(5)	11.2123(2)
c/Å	8.4738(2)	44.5065(13)	19.7023(3)
β/°	90	90	94.658(2)
V/Å^3	4415.4(2)	11 232.3(6)	4283.44(10)
Z	4	8	4
D_c/Mg m^{-3}	1.16	1.16	1.199
Absorption coefficient/mm^{-1}	0.33	0.28	0.343
θ Range for data collection/°	3.92–25.96	3.71–21.97	3.71–25.73
Reflections collected	14 970	48 346	35 268
Independent reflections	3706 (R_{int} = 0.072)	12 794 (R_{int} = 0.157)	7830 (R_{int} = 0.048)
Reflections with $I > 2\sigma(I)$	2900	6842	6626
Data/restraints/parameters	3706/1/235	12 794/721/1223	7830/0/468
Goodness-of-fit on F^2	1.034	0.980	0.993
Final *R* indices [$I > 2\sigma(I)$]	R_1 = 0.039, wR_2 = 0.080	R_1 = 0.068, wR_2 = 0.127	R_1 = 0.036, wR_2 = 0.086
R indices (all data)	R_1 = 0.061, wR_2 = 0.091	R_1 = 0.161, wR_2 = 0.158	R_1 = 0.048, wR_2 = 0.092
Largest diff. peak and hole/e Å^{-3}	0.31 and −0.43	0.39 and −0.51	0.33 and −0.52

Table 2 Crystal structure and refinement data for **4** and **5**

	4	**5**
Formula	$C_{50}H_{63}B_2N_3O_2Ti$ (½ C_6H_{14})	$C_{52}H_{65}N_3O_2Ti$
Formula weight	850.64	811.97
Temperature/K	173(2)	173(2)
Wavelength/Å	0.71073	0.71073
Crystal size/mm	0.3 × 0.25 × 0.25	0.4 × 0.4 × 0.15
Crystal system	Triclinic	Triclinic
Space group	$P\bar{1}$ (no. 2)	$P\bar{1}$ (no. 2)
a/Å	11.7856(6)	10.5789(1)
b/Å	11.9638(4)	19.5500(3)
c/Å	17.5685(9)	22.5063(3)
α/°	93.029(3)	82.370(1)
β/°	98.130(2)	89.957(1)
γ/°	91.726(3)	83.821(1)
V/Å^3	2447.1(2)	4586.3(1)
Z	2	4
D_c/Mg m^{-3}	1.15	1.18
Absorption coefficient/mm^{-1}	0.22	0.23
θ Range for data collection/°	4.12–25.01	3.75–24.76
Reflections collected	14 981	60 894
Independent reflections	8545 (R_{int} = 0.043)	15 458 (R_{int} = 0.071)
Reflections with $I > 2\sigma(I)$	6318	11 334
Data/restraints/parameters	8545/4/565	15 458/0/1061
Goodness-of-fit on F^2	1.018	1.102
Final *R* indices [$I > 2\sigma(I)$]	R_1 = 0.062, wR_2 = 0.146	R_1 = 0.065, wR_2 = 0.136
R indices (all data)	R_1 = 0.090, wR_2 = 0.162	R_1 = 0.098, wR_2 = 0.148
Largest diff. peak and hole/e Å^{-3}	0.77 and −0.58	0.47 and −0.36

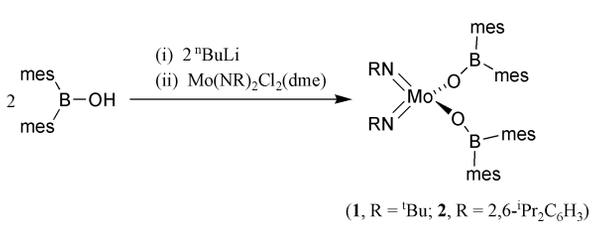

(**1**, R = ^{t}Bu; **2**, R = 2,6-^{i}Pr$_2$C$_6$H$_3$)

Scheme 1

bonding parameters in **1** and **2**, in particular the bonding within the Mo–B–O linkage, X-ray structural analyses were performed. The molecular structures are illustrated in Figs. 2 and 3, crystal data are summarised in Table 1 and selected bond lengths and angles are collected in Tables 3 and 4.

Compound **1** crystallises from hexane as the monomeric species, Mo(N^{t}Bu)$_2$[OB(mes)$_2$]$_2$, with a pseudo-tetrahedral arrangement of ligands around the molybdenum centre [inter-ligand angles in the range 106.48(14)–111.83(14)°]. The Mo–N bond length [1.726(3) Å] lies towards the lower end of the range typically found in d^0-bis(imido) molybdenum complexes,[13] which may reflect an increase in π-electron donation to a more electron deficient metal centre (*vide infra*). The N_{imido} angle

Table 3 Selected bond lengths (Å) and angles (°) for Mo(N^{t}Bu)$_2$[OB(mes)$_2$]$_2$ (**1**)

Mo–N	1.726(3)	Mo–O	1.914(2)
B–O	1.353(5)		
N–Mo–N′	110.0(3)	N–Mo–O	111.83(14)
O–Mo–O′	110.33(17)	N–Mo–O′	106.48(14)
Mo–N–C(1)	162.2(4)	Mo–O–B	155.5(3)

Symmetry elements: ′ $-x, -y, z$.

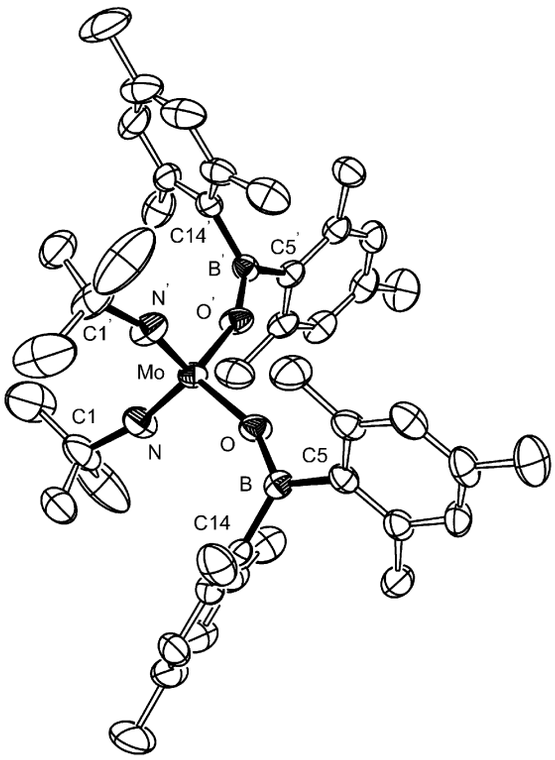

Fig. 2 Molecular structure of $Mo(N^tBu)_2[OB(mes)_2]_2$ (**1**) with thermal ellipsoids drawn at the 50% probability level. Hydrogen atoms omitted for clarity.

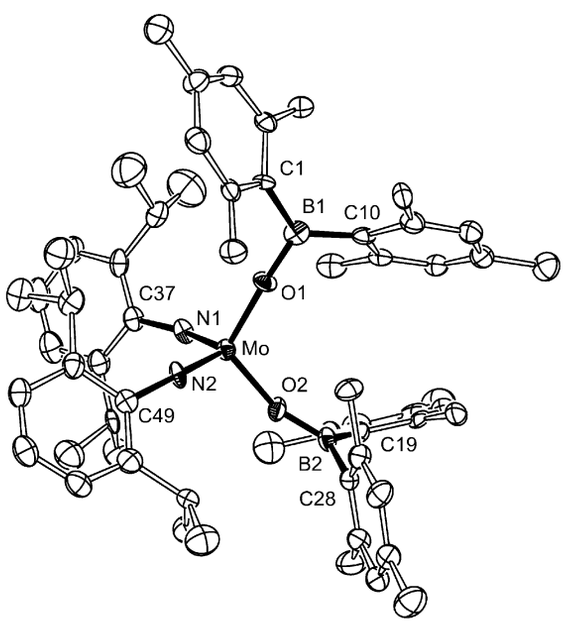

Fig. 3 Molecular structure of $Mo(NAr)_2[OB(mes)_2]_2$ (**2**) with thermal ellipsoids drawn at the 50% probability level. Hydrogen atoms omitted for clarity.

[162.2(4) Å] is, however, unremarkable, being in the range typical of terminal, 4-electron donor imido ligands.[13] The Mo–O bond length [1.914(2) Å] is longer than in the related four-coordinate bis(*tert*-butylimido)molybdenum complex, $[Mo(N^tBu)_2\{O(Ph_2SiO)_2\}]_2$,[14] [Mo–O = 1.899(6) and 1.873(6) Å] suggestive of a lower Mo–O bond order, predicted if π-electron density is being donated to the boron atom. However, the B–O bond length in **1** [1.353(5) Å] is not significantly shortened when compared with the parent borinic acid [1.367(6) Å].[4]

Table 4 Selected bond lengths (Å) and angles (°) for $Mo(NAr)_2[OB(mes)_2]_2$ (**2**).

Mo–N(1)	1.745(6)	Mo–N(2)	1.737(6)
	1.714(7)		1.746(7)
Mo–O(1)	1.870(5)	Mo–O(2)	1.883(5)
	1.887(5)		1.899(6)
O(1)–B(1)	1.338(11)	O(2)–B(2)	1.361(11)
	1.358(11)		1.352(12)
N(1)–Mo–N(2)	106.8(3)	N(1)–Mo–O(1)	108.2(3)
	108.7(3)		107.1(3)
O(1)–Mo–O(2)	113.1(2)	N(1)–Mo–O(2)	108.5(3)
	114.1(2)		107.7(3)
N(2)–Mo–O(1)	109.6(3)	N(2)–Mo–O(2)	110.5(3)
	109.2(3)		110.0(3)
Mo–N(1)–C(37)	154.7(6)	Mo–O(1)–B(1)	174.5(6)
	155.3(6)		170.4(6)
Mo–N(2)–C(49)	163.4(6)	Mo–O(2)–B(2)	158.4(6)
	160.7(7)		158.0(6)

Figures (one below the other) correspond to two crystallographically independent molecules.

The bis(arylimido) analogue (**2**) crystallises with two independent molecules in the unit cell, each of which adopt distorted tetrahedral geometry at the metal centre, with inter-ligand angles in the range 106.8(3)–113.1(2)° {107.1(3)–114.1(2)°} (values in { } refer to the second independent molecule). The Mo–N bond lengths of 1.737(6) and 1.745(6) Å {1.714(7) and 1.746(7) Å} are on average longer than in **1**, a likely consequence of π-delocalisation into the aromatic ring of the aryl substituent, while the Mo–N–C angles of 154.7(6) and 163.4(6)° {155.3(6) and 160.7(7)°} are again within the range associated with 'linear' imido ligands.[13] The Mo–O bond lengths of 1.883(5) and 1.870(5) Å {1.899(6) and 1.887(5) Å} are notably shorter than in **1**, implying an increase in π-donation from the oxygen lone-pairs, which may compensate for the reduced electron donation from the arylimido substituents. One of the boroxide oxygens in each molecule is considerably more bent 158.4(6)° {158.0(6)°} than the other 174.5(6)° {170.4(6)°}, although this has little effect on the corresponding Mo–O bond length. In addition the B–O distances within the 'bent' 1.361(11) Å {1.352(12) Å} and 'linear' 1.338(11) Å {1.358(11) Å} boroxide ligands do not appear to follow any predictable trend, suggesting that steric factors are also contributing to the overall molecular structure.

In an attempt to evaluate the impact of the boron atom on the metal–oxygen bonding in **1** and **2**, we sought other molybdenum bis(imido)bis(alkoxide) complexes with which to compare bond parameters. However, the relative dearth of structurally characterised examples became apparent, and hence we embarked on the synthesis of compounds of general formula $Mo(NR)_2(OR')_2$. To maximise the validity of any comparison in terms of the electronic effect of the boron atom, we targeted an alkoxide incorporating similarly sized substituents to the $[(mes)_2BO]^-$ ligand used in **1** and **2**. Accordingly dimesitylmethanol, $(mes)_2CHOH$, was prepared according to literature procedures,[9] and investigated as an alkoxide ligand precursor in molybdenum bis(imido) chemistry.

Deprotonation of the alcohol proceeds in Et_2O at 0 °C using ^{n}BuLi, to afford a white precipitate, presumed to be the ether adduct $[(mes)_2CHOLi(Et_2O)_n]_x$ (Scheme 2). We again found it

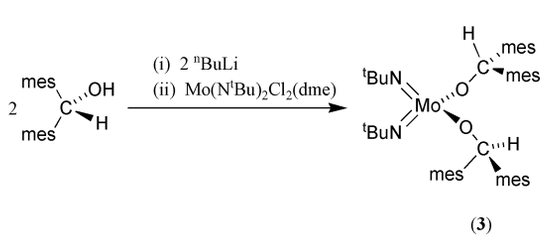

(**3**)

Scheme 2

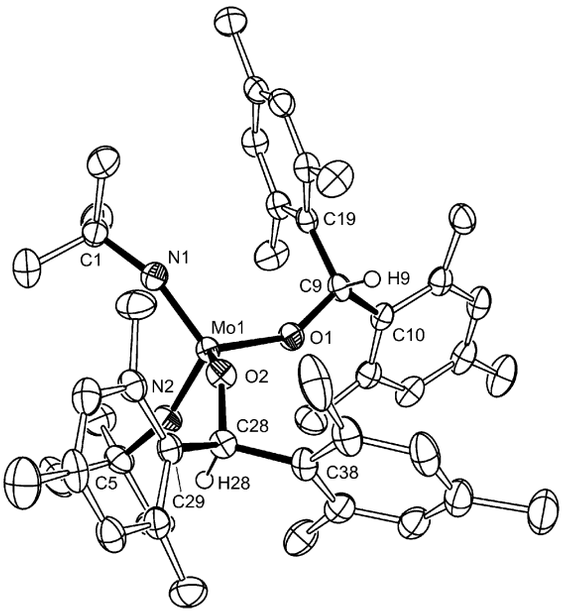

Fig. 4 Molecular structure of $Mo(N^tBu)_2[OCH(mes)_2]_2$ (**3**) with thermal ellipsoids drawn at the 50% probability level. Hydrogen atoms, except for C*H*$(mes)_2$, omitted for clarity.

Table 5 Selected bond lengths (Å) and angles (°) for $Mo(N^tBu)_2[OCH(mes)_2]_2$ (**3**)

Mo–N(1)	1.742(2)	Mo–N(2)	1.740(2)
Mo–O(1)	1.8930(16)	Mo–O(2)	1.9089(16)
N(1)–Mo–N(2)	110.27(10)	N(1)–Mo–O(1)	112.62(8)
O(1)–Mo–O(2)	113.34(7)	N(1)–Mo–O(2)	106.62(8)
N(2)–Mo–O(1)	105.86(8)	N(2)–Mo–O(2)	108.07(8)
Mo–N(1)–C(1)	160.41(18)	Mo–O(1)–C(9)	144.99(15)
Mo–N(2)–C(5)	162.78(18)	Mo–O(2)–C(28)	131.69(14)

most convenient to proceed without isolation of the Li-salt, and hence addition of a slurry of two equivalents of the Li-salt to a cooled (−78 °C) solution of $Mo(N^tBu)_2Cl_2$(dme) afforded, after the appropriate work-up, the compound $Mo(N^tBu)_2[OCH(mes)_2]_2$ (**3**). Cooling a saturated hexane solution of **3** to −30 °C afforded colourless crystals suitable for an X-ray analysis. The molecular structure is illustrated in Fig. 4, crystal data are summarised in Table 1 and selected bond lengths and angles are collected in Table 5.

Compound **3** also exists as a monomeric, distorted tetrahedral complex, with bond lengths and angles in the range 105.86(8)–113.34(7)°. Whilst a greater distortion from ideal tetrahedral geometry exists when compared with **1**, the differences are deemed sufficiently small to permit reasonable comparisons to be made between the corresponding bond lengths and angles. It is also noted that although the two complexes crystallise in different space groups (**1**, orthorhombic; **3**, monoclinic), no intermolecular contacts are present in either structure. While detailed cone angle measurements have not been conducted, space filling models generated from the crystal data for **1** and **3** illustrate the correlation that exists between the steric demands of the $[OB(mes)_2]^-$ and $[OCH(mes)_2]^-$ ligands (Fig. 5). However, it is noted that such considerations should be treated as a first approximation, as a slightly larger O–Mo–O angle is observed in **3** [113.34(7) °] than in **1** [110.33(17)°], which reflects the different projection of the mesityl substituents that results from changing a trigonal planar boron atom (Σ_{angles} in **1** and **2** = 360 ± 0.2°) to a tetrahedral carbon in **3**.

The Mo–N bond distances in **3** [1.742(2) and 1.740(2) Å] are notably longer than in the analogous *tert*-butylimido compound **1**, suggestive of a reduction in π-donation to the molybdenum centre. The Mo–N–C angles in **3** [160.41(18) and 162.78(18)°], however, do not exhibit any significant bending compared with the corresponding angle in **1** [162.2(4)°]. The Mo–O distances [1.8930(16) and 1.9089(16) Å] are shorter than in **1**, consonant with greater π-donation from the oxygen to the Mo-centre. The angles at the O-atoms [144.99(15) and 131.69(14)°] are considerably more bent than in the boroxide ligands of **1**, which may indicate that the π-electrons are distributed across the three atoms of the 'Mo–O–B' moiety in **1**, while in **3** they are localised to a greater extent in the Mo–O bond.

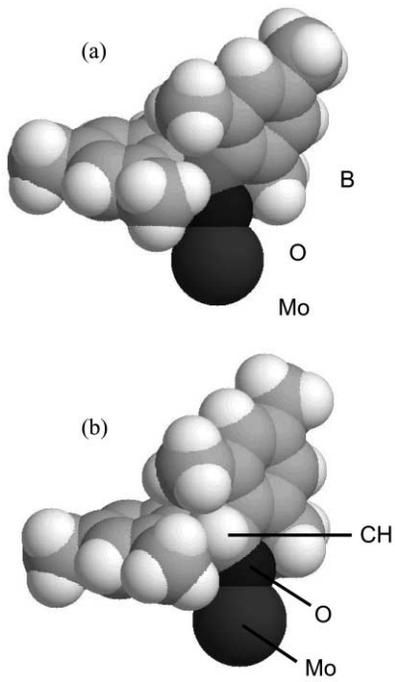

Fig. 5 Space filling representation of $[(mes)_2BO]^-$ and $[(mes)_2CHO]^-$. Crystal data taken from compounds **1** and **3** respectively.

In summary, the molybdenum–nitrogen and molybdenum–oxygen bond lengths show the changes predicted if the boroxide ligand is acting as a less effective π-donor to the metal centre; comparison of the analogous compounds **1** and **3** therefore reveals shorter imido and longer alkoxide bonds in the boron-containing complex. However, the relative angles at nitrogen and oxygen do not clearly support these observations, highlighting the 'soft' nature of the metal–imido and metal–alkoxide bonds. We conclude that, although care has been taken to maximise the structural similarities between the complexes, steric interactions may still play an important role that needs to be considered when comparing bond lengths and angles.

To elucidate further the role that sterics play in the arrangement of the ligand substituents, we initiated a study of the related *tert*-butylimido complexes of titanium that, on the basis of previously reported aryloxide derivatives,[15] were predicted to display a different coordination geometry at the metal centre. Thus, reaction between two equivalents of the lithium salt of $(mes)_2BOH$ or $(mes)_2CHOH$, prepared as described above, and the ubiquitous titanium imido starting material, $[Ti(N^tBu)Cl_2(py)_3]$,[11] afforded the compounds $Ti(N^tBu)[OB(mes)_2]_2(py)_2$ (**4**) and $Ti(N^tBu)[OCH(mes)_2]_2(py)_2$ (**5**) respectively (Scheme 3). NMR data and combustion analysis were consistent with a monomeric, five-coordinate mono(imido)bis(alkoxide) structure retaining two equivalents of pyridine per titanium. Mass spectral analysis of complex **4**, however, was consistent with a higher nuclearity cluster, conceivably occurring through either bridging imido or alkoxide groups. To determine the bonding present in the solid state, and compare the bond parameters of the ligands, X-ray structural analyses were performed on **4** and **5**. The molecular structures are illustrated in Figs. 6 and 7,

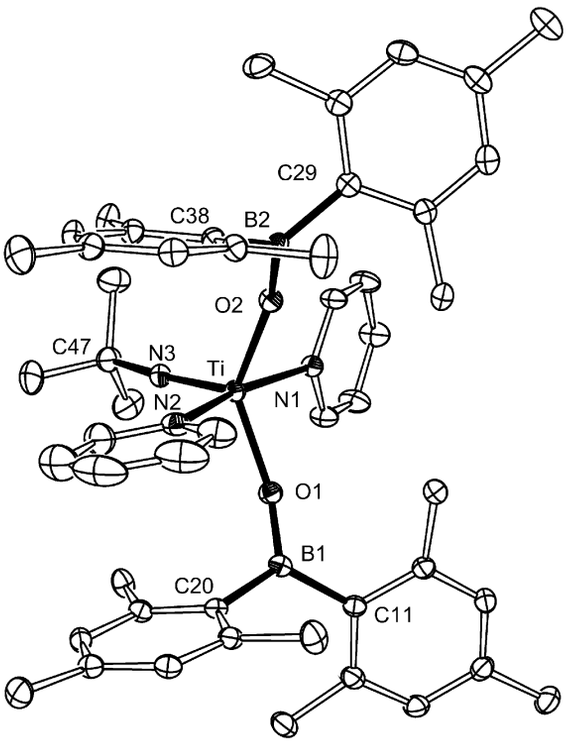

Fig. 6 Molecular structure of Ti(N^{t}Bu)[OB(mes)$_2$]$_2$(py)$_2$ (**4**) with thermal ellipsoids drawn at the 50% probability level. Hydrogen atoms omitted.

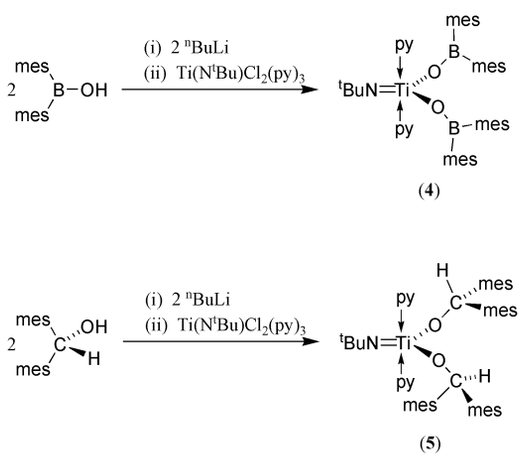

Scheme 3

crystal data are summarised in Table 2 and selected bond lengths and angles are collected in Tables 6 and 7.

Both complexes **4** and **5** exist as monomeric species in the solid state, each with a terminal imido, two alkoxide/boroxide ligands and two donor pyridine molecules. This suggests that the higher peaks in the mass spectra are an artifact generated from combination of molecular fragments that most likely occur upon loss of pyridine. Compound **5** is present as two independent molecules in the unit cell (values in { } refer to the second molecule). The five-coordinate Ti centre in **4** is virtually midway between a trigonal bipyramid and square-based pyramid, as defined by the τ value of 0.57.[16] In contrast, **5** is much closer to true trigonal bipyramidal geometry with $\tau = 0.78$ {$\tau = 0.79$}, arising primarily from a significant reduction in the O–Ti–O bond angle from 133.50(9)° in **4** to 123.24(10)° {123.25(10)°} in **5**, with a commensurate increase in the N_{imido}–Ti–O angles.

The Ti=N_{imido} distance for **4** [1.706(3) Å] is unchanged from the starting material,[11] with a Ti–N–C angle [169.4(2)°] typical for a linear, 4-electron donor group. Although no significant

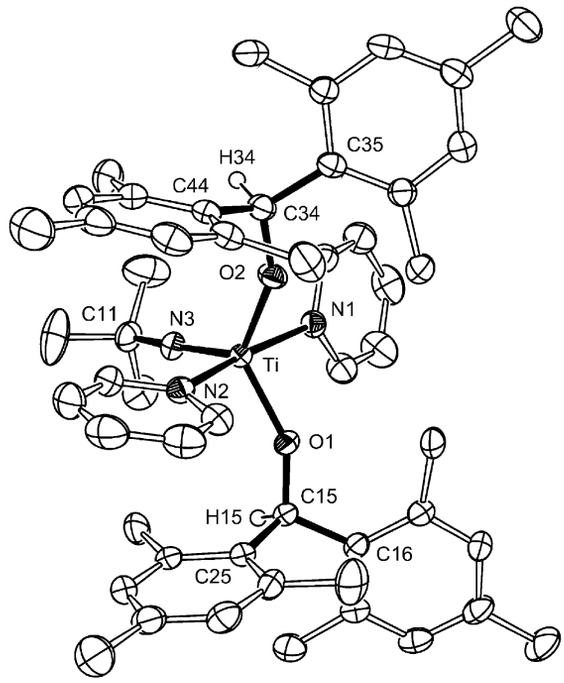

Fig. 7 Molecular structure of Ti(N^{t}Bu)[OCH(mes)$_2$]$_2$(py)$_2$ (**5**) with thermal ellipsoids drawn at the 50% probability level. Hydrogen atoms, except for C*H*(mes)$_2$, omitted for clarity.

Table 6 Selected bond lengths (Å) and angles (°) for Ti(N^{t}Bu)[OB(mes)$_2$]$_2$(py)$_2$ (**4**)

Ti–N(3)	1.706(3)	Ti–O(1)	1.925(2)
Ti–N(1)	2.246(2)	Ti–O(2)	1.934(2)
Ti–N(2)	2.236(3)	O(1)–B(1)	1.332(4)
		O(2)–B(2)	1.331(4)
N(1)–Ti–N(2)	167.95(10)	O(1)–Ti–O(2)	133.50(9)
N(1)–Ti–N(3)	91.86(10)	O(2)–Ti–N(1)	88.92(8)
N(2)–Ti–N(3)	100.14(11)	O(2)–Ti–N(2)	87.42(9)
O(1)–Ti–N(1)	87.55(8)	O(2)–Ti–N(3)	113.26(11)
O(1)–Ti–N(2)	86.66(9)	Ti–O(1)–B(1)	159.91(19)
O(1)–Ti–N(3)	113.19(11)	Ti–O(2)–B(2)	158.92(19)
Ti–N(3)–C(47)	169.4(2)		

Table 7 Selected bond lengths (Å) and angles (°) for Ti(N^{t}Bu)[OCH(mes)$_2$]$_2$(py)$_2$ (**5**)

Ti–N(3)	1.715(3)	O(2)–C(34)	1.402(4)
	1.716(3)		1.405(4)
Ti–O(1)	1.887(2)	C(15)–C(16)	1.539(4)
	1.889(2)		1.541(4)
Ti–O(2)	1.872(2)	C(15)–C(25)	1.540(4)
	1.875(2)		1.541(4)
Ti–N(1)	2.271(3)	C(34)–C(35)	1.544(4)
	2.258(3)		1.537(4)
Ti–N(2)	2.247(3)	C(34)–C(44)	1.545(5)
	2.243(3)		1.542(5)
O(1)–C(15)	1.403(3)	N(3)–C(11)	1.458(4)
	1.404(4)		1.453(4)
N(1)–Ti–N(2)	170.32(10)	Ti–O(1)–C(15)	149.44(19)
	170.42(10)		147.27(19)
N(3)–Ti–O(1)	118.21(11)	Ti–O(2)–C(34)	151.8(2)
	117.39(11)		152.6(2)
N(3)–Ti–O(2)	118.29(11)	Ti–N(3)–C(11)	167.8(2)
	119.08(11)		167.7(2)
O(1)–Ti–O(2)	123.24(10)	O(1)–C(15)–C(16)	114.7(2)
	123.25(10)		114.9(2)
N(3)–Ti–N(1)	90.58(11)	O(2)–C(34)–C(35)	114.6(3)
	90.37(11)		114.5(3)

Figures (one below the other) correspond to two crystallographically independent molecules.

Table 8 $\Delta\delta$ Values for complexes of general formula $Mo(N^tBu)_2X_2$. Spectra recorded in C_6D_6 unless otherwise stated

X	α	β	$\Delta\delta$	Ref.
Cl	74.1	30.1	41.6	19
$OB(mes)_2$	71.0	31.6	39.4	This work
$OCH(mes)_2$	69.6	32.4	37.2	This work
$OSiMe_3$ [a]	68.8	32.2	36.6	18
O^tBu	67.9	[b]	35.6	20
NH^tBu	67.2	32.8	34.4	20

[a] Spectrum recorded in d_8-toluene. [b] The two peaks for the β-carbons (δ 32.4 and 32.2) corresponding to the O^tBu and N^tBu were unassigned – the $\Delta\delta$ was therefore calculated from an average value.

reduction in the $Ti{=}N_{imido}$ distance is observed on replacing the boroxide ligands with 'conventional' hydrocarbon alkoxide groups in **5** [1.715(3) Å {1.716(3) Å}], a slight decrease in the Ti–N–C angle to 167.8(2)° {167.7(2)°} is noted, consistent with an increase in the π-electron density at the nitrogen atom (*vide infra* for spectroscopic analysis). The Ti–O bonds in **4** [1.925(2) and 1.934(2) Å] are longer than in **5** [1.872(2) and 1.887(2) Å; {1.889(2) and 1.875(2) Å}], and notably larger than in other, related titanium(imido) aryloxide complexes.[15,17] This is again consistent with a reduction in π-donation to Ti from the boroxide ligand, also supported by a reduction in the B–O bond lengths 1.332(4) and 1.331(4) Å. In addition, the angles at the oxygen atom in **4** [159.91(19) and 158.92(19)°] are significantly closer to linearity than the corresponding angles in **5** [149.44(19) and 151.8(2)°; {147.27(19) and 152.6(2)°}], suggesting possible delocalisation across the Ti–O–B fragment.

Previous work on d^0-*tert*-butylimido complexes have established a correlation between the chemical shift difference of the α and β-carbon atoms ($\Delta\delta$), and the electron density of the imido nitrogen atom.[18] Table 8 displays $\Delta\delta$ values for **1** and **3** along with data taken from related complexes of general formula $Mo(N^tBu)_2X_2$. Generally we observe that the lower the electron donating ability of the X-ligand, the larger the $\Delta\delta$ value corresponding to a reduction in electron density at the N_{imido} atom. Thus the value for **1** ($\Delta\delta$ = 39.4) is in agreement with the boroxide ligand behaving as a relatively poor electron donor to the molybdenum centre, with a value similar to that observed for in the dichloride complex ($\Delta\delta$ = 41.6). The value for **3** ($\Delta\delta$ = 37.2) is in the range observed for related siloxide and alkoxide complexes, with the slightly higher value a possible reflection of the electron withdrawing nature of the mesityl substituents.

Comparing the $\Delta\delta$ values for **4** and **5** with a range of d^0-titanium mono(imido) complexes we see a similar trend to that observed for the molybdenum bis(imido) species (Table 9). Thus, as the electron density at titanium increases through introduction of more donor groups to the metal centre, the corresponding $\Delta\delta$ value decreases, as illustrated by the relative values of $Ti(N^tBu)Cl_2(py)_2$ ($\Delta\delta$ = 42.8) *vs.* $Ti(N^tBu)Cl_2(py)_3$ ($\Delta\delta$ = 41.5), and $[Ti(N^tBu)(OAr)_2]_2$ ($\Delta\delta$ = 40.2) *vs.* $Ti(N^tBu)(OAr)_2(py)_2$ ($\Delta\delta$ = 37.0) (Ar = 2,6-$Me_2C_6H_3$). The value for **4** ($\Delta\delta$ = 38.0) is slightly greater than that for related aryloxide complexes with two donor pyridine molecules ($\Delta\delta$ = 37.0–35.7), suggesting similar donor properties. As predicted, compound **5** has a lower value ($\Delta\delta$ = 35.0) implying a higher electron density at the imido nitrogen that arises from the alkoxide ligand behaving as a better π-donor to the d^0-metal centre. The data taken from both systems is therefore in agreement with the original proposal that the boroxide ligand behaves electronically as an 'electron-deficient' alkoxide. We are currently investigating the differences in the chemistry associated with the boron-substituted ligand in comparison with the hydrocarbon analogues.

Table 9 $\Delta\delta$ Values for complexes of general formula $Ti(N^tBu)X_2(donor)_n$. Spectra recorded in $CDCl_3$ unless otherwise stated

X	$(donor)_n$	α	β	$\Delta\delta$	Ref.
Cl	$(py)_2$	73.1	30.3	42.8	11
Cl	$(py)_3$	71.5	30.0	41.5	11
OAr [a]	—	73.3	33.1	40.2	15
$OB(mes)_2$	$(py)_2$	69.6	31.6	38.0	This work
OAr′	$(py)_2$	68.8	31.7	37.1	15
OAr	$(py)_2$	68.7	31.7	37.0	15
OAr″	$(py)_2$	72.1	35.4	36.7	15
OAr′	$(py')_2$	68.0	32.3	35.7	17*b*
$OCH(mes)_2$	$(py)_2$	67.1	32.1	35.0	This work

[a] Complex is dimeric in the solid state, with bridging *tert*-butylimido ligands. Ar = 2,6-$Me_2C_6H_3$; Ar′ = 2,6-$^iPr_2C_6H_3$; OAr″ = 2,6-$^tBu_2C_6H_3$; py′ = 4-pyrrolidinopyridine.

Acknowledgements

We thank the EPSRC for a research studentship (S. C. C.) and University of Sussex for additional financial support. We would like to thank Professor V. C. Gibson and Dr E. L. Marshall for providing the ^{13}C spectroscopic data for $Mo(N^tBu)_2(O^tBu)_2$ and $Mo(N^tBu)_2(NH^tBu)_2$. We also wish to acknowledge the use of the EPSRC's Chemical Database Service at Daresbury.

References

1 D. C. Bradley, R. C. Mehrotra and D. P. Gaur, *Metal Alkoxides*, Academic, New York, 1978; R. C. Mehrotra, *Adv. Inorg. Chem.*, 1983, **26**, 269; I. P. Rothwell, *Acc. Chem. Res.*, 1988, **21**, 153.
2 V. C. Gibson, *J. Chem. Soc., Dalton Trans.*, 1994, 1607; V. C. Gibson, *Angew. Chem., Int. Ed. Engl.*, 1994, **33**, 1565.
3 R. R. Schrock, *Polyhedron*, 1995, **14**, 3177; W. J. Feast, V. C. Gibson and E. L. Marshall, *J. Chem. Soc., Chem. Commun.*, 1992, 1157; R. R. Schrock, *Tetrahedron*, 1999, **55**, 8141.
4 K. J. Weese, R. A. Bartlett, B. D. Murray, M. M. Olmstead and P. P. Power, *Inorg. Chem.*, 1987, **26**, 2409.
5 H. Chen, P. P. Power and S. C. Shoner, *Inorg. Chem.*, 1991, **30**, 2884.
6 V. C. Gibson, C. Redshaw, W. Clegg and M. R. Elsegood, *Polyhedron*, 1997, **16**, 2637.
7 J. E. Balkwill, S. C. Cole, M. P. Coles and P. B. Hitchcock, *Inorg. Chem.*, 2002, **41**, 3548.
8 H. C. Brown and V. H. Dodson, *J. Am. Chem. Soc.*, 1957, **79**, 2302.
9 S. Grilli, L. Lunazzi, A. Mazzanti, D. Casarini and C. Femoni, *J. Org. Chem.*, 2001, **66**, 488.
10 A. Bell, W. Clegg, P. W. Dyer, M. R. J. Elsegood, V. C. Gibson and E. L. Marshall, *J. Chem. Soc., Chem. Commun.*, 1994, 2547.
11 A. J. Blake, P. E. Collier, S. C. Dunn, W.-S. Li, P. Mountford and O. V. Shishkin, *J. Chem. Soc., Dalton Trans.*, 1997, 1549.
12 G. M. Sheldrick, SHELXL-97, Program for the Refinement of Crystal Structures, University of Göttingen, Germany, 1997.
13 D. E. Wigley, *Prog. Inorg. Chem.*, 1994, **42**, 239; W. A. Nugent and B. L. Haymore, *Coord. Chem. Rev.*, 1980, **31**, 123; W. A. Nugent and J. M. Mayer, *Metal–Ligand Multiple Bonds*, Wiley, New York, 1988.
14 L. King, M. Motevalli and A. C. Sullivan, *J. Chem. Soc., Dalton Trans.*, 2000, 1357.
15 P. E. Collier, A. J. Blake and P. Mountford, *J. Chem. Soc., Dalton Trans.*, 1997, 2911.
16 A. W. Addison, T. N. Rao, J. Reedijk, J. van Rijn and G. C. Verschoor, *J. Chem. Soc., Dalton Trans.*, 1984, 1349.
17 (*a*) C. H. Zambrano, R. D. Profilet, J. E. Hill, P. E. Fanwick and I. P. Rothwell, *Polyhedron*, 1993, **12**, 689; (*b*) J. E. Hill, R. D. Profilet, P. E. Fanwick and I. P. Rothwell, *Angew. Chem., Int. Ed. Engl.*, 1990, **29**, 664.
18 W. A. Nugent, R. J. McKinney, R. V. Kasowski and F. A. van-Catledge, *Inorg. Chim. Acta*, 1982, **65**, L91.
19 G. Schoettel, J. Kress and J. A. Osborn, *J. Chem. Soc., Chem. Commun.*, 1989, 1062.
20 M. Jolly, Ph.D. Thesis, Durham University, Durham, UK, 1994.